Computer-based Assessment of the Effects of Amiodarone on Short QT Syndrome Variant 1 in Human Ventricles

Cunjin Luo[1,2], Kuanquan Wang[1], Yang Liu[1], Yong Xia[3], Henggui Zhang[1,2,4,5]

[1] School of Computer Science and Technology, Harbin Institute of Technology, Harbin, China
[2] Key Laboratory of Medical Electrophysiology, Ministry of Education, Collaborative Innovation Centre for Prevention and Treatment of Cardiovascular Disease/Institute of Cardiovascular Research, Southwest Medical University, Luzhou, China
[3] School of Computer Science and Technology, Harbin Institute of Technology, Weihai, China
[4] Space Institute of Southern China, Shenzhen, China
[5] School of Physics and Astronomy, The University of Manchester, Manchester, United Kingdom

Abstract

Short QT syndrome (SQTS) is a channelopathy associated with a short QT interval and an increased risk of arrhythmias. The SQT1 variant results from a gain-of-function mutation (N588K) in the KCNH2-encoded channels. Inherited arrhythmogenic effects of SQTS have been clearly characterized, while little is known about the pharmacological therapy for SQTS. Therefore, this paper assessed the effects of amiodarone, class III anti-arrhythmic agent, on SQT1. The wild-type (WT) and N588K I_{Kr} Markov chain formulations were incorporated into human ventricular action potentials (APs). The modified cells were then integrated into one-dimensional (1D) and 2D tissues. The inhibitory effect of amiodarone on channels was modelled using half-maximal inhibitory concentration (IC_{50}) and Hill coefficient (nH) values. Amiodarone prolonged the SQT1 ventricular cell AP duration (APD). Amiodarone caused a QT prolongation and a decrease in T-wave amplitude. Amiodarone decreased vulnerable window, and increased the critical size of ventricular substrates. Amiodarone terminated and prevented re-entrant waves. The actions of amiodarone exhibited in silico, that anti-arrhythmic effects on SQT1. Our data substantiate a causal link between amiodarone and QT interval prolongation, and offer an explanation for decreased vulnerability to re-entry and termination of re-entrant arrhythmias in SQT1.

1. Introduction

'Short QT syndrome' (SQTS) is an identified cardiac channelopathy associated with abnormally short QT intervals and increased risk of arrhythmia generation. The first identified SQTS (SQT1 variant) was identified in a 51-year-old male presenting a corrected QT interval (QTc) of 288 ms on the electrocardiogram (ECG) [1]. A pair of bases substituted from asparagine to lysine at position 588 (N588K) in the S5-pore linker region of the KCNH2-encoded potassium channel was discovered. The results from in vitro voltage clamp recordings have shown that N588K mutation leads to a loss of normal rectification of rapid delayed rectifier potassium current (I_{Kr}), resulting in a gain-of-function during the late repolarization of the action potential (AP) in cardiomyocytes. The current treatment for SQTS patients is the application of an implantable cardioverter defibrillator (ICD), but the use of ICD does not restore the QT interval. To treat SQTS patients, pharmacological therapy may restore the normal QT interval and protect against malignant arrhythmias. As QT shortening is attributable to abbreviated APs secondary to an increase in I_{Kr}, blocking N588K channels could be an effective treatment of SQT1 patients. However, data regarding pharmacological treatment in SQT1 are very limited. A clinical study by Lu et al. presented that amiodarone prevented the incidence of arrhythmia and prolonged the QT interval in an SQTS patient, but clinical data were not available in that patient [2].

The aim of this study was to use biophysically computer-based modelling to assess the effects of amiodarone on the electrical properties of human myocardium in SQT1. Specifically, we investigated whether experimentally-determined changes in these ion currents could account for the changes in AP and the transmural heterogeneity in APD. In addition, we investigated how such ionic and cellular changes influenced pseudo-ECGs, excitation wave conduction and temporal susceptibility to the initiation of re-entry. To achieve this we constructed a one-dimensional (1D) model of ventricular myocytes. These strands were then combined together to create a two-dimensional (2D)

 ISSN: 2325-887X DOI:10.22489/CinC.2017.181-145

transmural sheet model to investigate the susceptibility to the maintenance of re-entry, and further understand whether or not amiodarone terminates re-entrant waves.

2. Methods

The human ventricular cell model developed by ten Tusscher et al. [3] was chosen for this study. The parameters of I_{Kr} equations in the original model were replaced with a Markov chain (MC) model of the wild-type (WT) and N588K I_{Kr} [4,5].

The reduction of the maximum channel conductance was determined by the half-maximal inhibitory concentration (IC_{50}) and Hill coefficient (nH) values reported previously (shown in Table 1). In this study, two concentrations of amiodarone in the effective therapeutic range (between 1 μM and 3 μM) were chosen. The resulting maximum channel conductivities relative to their original values in the presence of amiodarone are provided in Table 2.

Table 1. Inhibition of cardiac ion currents in the presence of amiodarone

	WT			N588K		
	IC_{50}	n_H	Source	IC_{50}	n_H	Source
I_{Kr}	0.0752	1.00	[6]	0.318	1.0	[6]
I_{Na}	4.84	0.76	[7]	4.84	0.76	[7]
I_{NaK}	15.60	1.00	[8]	15.60	1.00	[8]
I_{CaL}	5.80	1.00	[9]	5.80	1.00	[9]
I_{NaCa}	3.30	1.00	[10]	3.30	1.00	[10]
I_{Ks}	3.84	0.63	[11]	3.84	0.63	[11]

Table 2. Effects of amiodarone on I_{Kr}, I_{Na}, I_{NaK}, I_{CaL}, I_{NaCa}, and I_{Ks} in the myocytes, expressed as a percentage of original value

	WT					
	G_{Kr}	G_{Na}	P_{NaK}	G_{CaL}	P_{NaCa}	G_{Ks}
1μM	7.00	76.33	93.98	85.29	76.74	69.42
3μM	2.44	58.78	83.87	65.91	52.38	53.73
	N588K					
1μM	24.13	76.33	93.98	85.29	76.74	69.42
3μM	9.59	58.78	83.87	65.91	52.38	53.73

Conduction of action potentials can be described by:

$$C_m \frac{\partial V_m}{\partial t} = -(I_{ion} + I_{stim}) + \nabla \cdot (D \nabla V_m) \quad (1)$$

where ∇ is the spatial gradient, and D is the diffusion coefficient. D was set to a value of 0.008 mm^2/ms.

The strand employed a spatial resolution of 0.15 mm and had 25 nodes for ENDO, 35 nodes for MIDDLE, and 40 nodes for EPI cells. To initiate a wave, a supra-threshold stimulus (amplitude: -52 pA/pF; duration: 1 ms) was applied to elicite an electrical wave. The pseudo-ECG was computed by the method of Gima and Rudy [12]. We placed the electrode at a position 2.0 cm away from the EPI end of the strand.

A 2D tissue was modelled by expanding the 1D transmural strand (15 mm) into a sheet with a width of 150 mm. Re-entry in a 2D tissue was initiated by an S1-S2 protocol. The S1 (amplitude: -52 pA/pF, duration: 1 ms) was applied to the ENDO layer to evoke a planar excitation wave. During the vulnerable window, an S2 with the same amplitude and duration as the S1 was applied to the MIDDLE-EPI junction. In order to evaluate the critical size of the re-entrant pathway, we estimated the minimum length of S2. The minimum length gives an inverse index of the susceptibility to re-entrant waves.

3. Results

Figure 1 exhibits the time course of AP, corresponding APD_{90}, and I_{Kr} profile/peak density in the presence of low and high doses of amiodarone. These results indicate: (i) the WT I_{Kr} increased during the time course of the initial AP phases, reaching the maximal amplitude before a rapid decrease during the late repolarization; (ii) the N588K I_{Kr} increased more rapidly following the AP upstroke, and reached a higher peak amplitude, leading to the APD abbreviation; (iii) both low and high doses of amiodarone prolonged the APD, and the effect of low-dose amiodarone on SQT1 AP was much closer to that in WT condition; (iv) both low and high doses of amiodarone markedly decreased the AP amplitude but did not affect the resting potential (RP).

We simulated the effect of amiodarone on the pseudo-ECG. The results are presented in Figure 2. EPI I_{Kr} was set to 1.6-fold greater than that in the MIDDLE and ENDO cells [13]. The pseudo-ECG show an increment in the QT interval caused by the application of low and high doses of amiodarone from 394 (control) in the WT condition to 446 and 460 ms, respectively. For the same condition, the QT interval was prolonged from 286 ms in the N588K condition to 398 and 436 ms, respectively. The QT interval in the low dose of amiodarone under N588K condition is 398 ms, which is within the normal range of QT between 363 and 421 ms. T-wave amplitude in the low dose amiodarone under N588K condition was decreased close to that in the WT control condition.

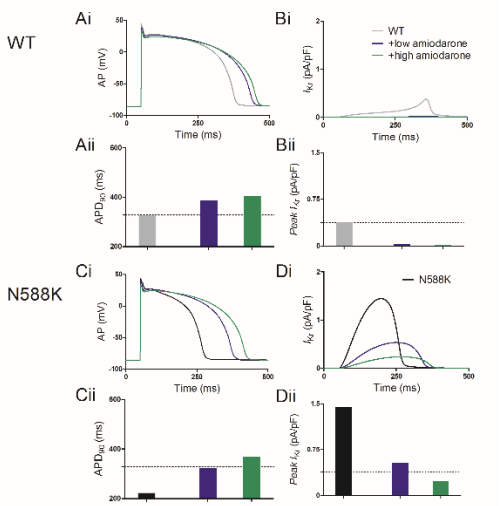

Figure 1. Effects of low and high doses of amiodarone on human ventricular ENDO AP (Ai and Ci) and APD90 (Aii and Cii), and I_{Kr} current profile (Bi and Di)/peak density (Bii and Dii) in WT and N588K conditions.

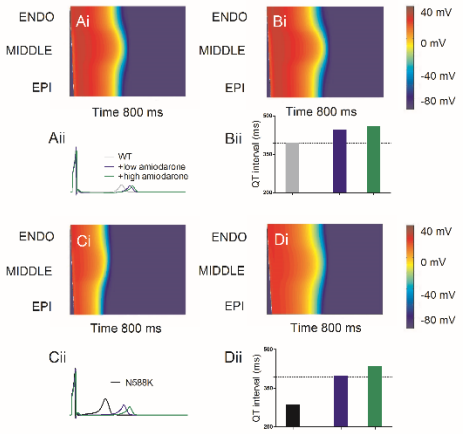

Figure 2. Plots of AP propagation, pseudo-ECG, and QT intervals. (Ai and Ci) Colour mapping of membrane potential. (Bi and Di) Colour mapping of membrane potential with the amiodarone. (Aii and Cii) Pseudo-ECGs. (Bii and Dii) QT intervals.

Amiodarone prolonged ERP and caused a rightward shift in the ERP restitution curves with increased maximal slopes in Figure 3. The premature stimulus was applied sufficiently early, within, and after the vulnerable window, bidirectional conduction block, unidirectional block, and bidirectional conduction were produced, respectively. The vulnerable window decreased from 1.5 ms in the WT condition to 1.3 and 0.8 ms in the use of low and high doses of amiodarone, respectively, and it decreased from 3.1 ms in the N588K condition to 1.5 and 1.3 ms, respectively.

We further proceeded to assess the effects of amiodarone on re-entry. The S1 was applied to evoke a wave. After a time delay, the premature stimulus (S2) during the vulnerable window produced unidirectional conduction block, as showed in Figure 4. Amiodarone terminated and prevented re-entry. A recording of the evolution of the AP of a cell was shown. The dominant frequency was from 4.8 Hz for WT to 4.6 and 4.3 Hz low-, and high-dose of amiodarone conditions, and was from 5.3 Hz for N588K to 4.8 and 4.5 Hz, respectively. Using the 2D tissue model we then quantified the minimum length of S2 that provides sufficient substrates to accommodate a re-entrant circuit. The spatial length of S2 was increased from 71 mm in WT to 75 and 79 mm in low- and high- dose amiodarone, respectively, and from 41 mm in N588K to 71 and 75 mm, respectively.

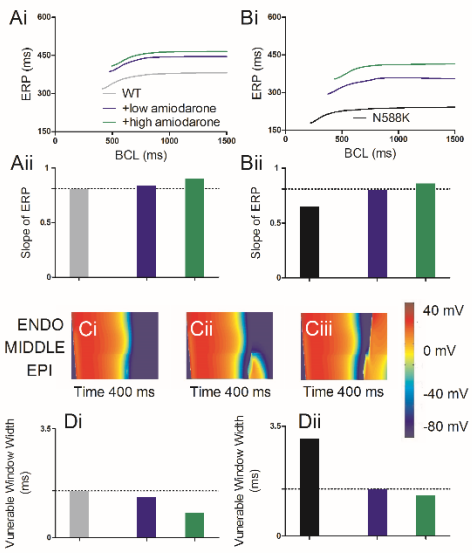

Figure 3. ERP restitution curves and vulnerable window. (Ai and Bi) ERP restitution curves. (Aii and Bii) Slopes of ERP restitution curves. (Ci, Cii, and Ciii) Plots of propagating wave. (Ci) Bidirectional conduction block. (Cii) Unidirectional conduction block. (Ciii) Bidirectional conduction. (Di and Dii) The vulnerable window width.

4. Conclusion

Our simulations indicate that amiodarone (i) caused prolongation of the APD; (ii) extended the QT interval on the computed pseudo-ECG; (iii) decreased the tissue' temporal vulnerability to genesis of unidirectional conduction block in response to a premature stimulus; (iv) terminated re-entrant excitation waves and increased the critical mass of ventricular substrate required to maintain re-entrant waves. These findings substantiate a causal link between the actions of amiodarone on the ion channel conductance and QT interval prolongation, and offer a potential explanation for decreased vulnerability of ventricular tissue to re-entry and termination of re-entrant arrhythmias in SQT1.

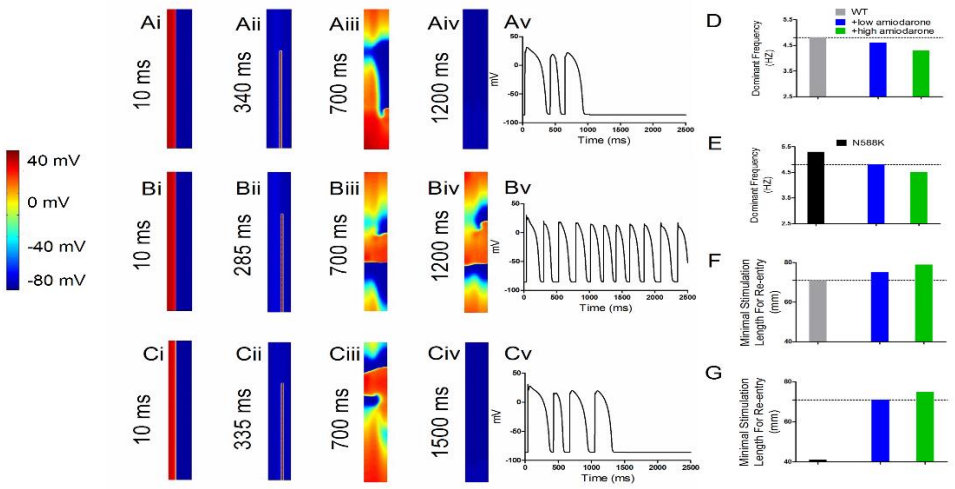

Figure 4. Snapshots of amiodarone effects on the initiation and conduction of re-entrant waves. (Ai, Bi, and Ci) A planar wave generated by S1. Snapshots at time = 10 ms. (Aii, Bii, and Cii) S2 applied to the local EPI region. (Aiii, Biii, and Ciii) Developed re-entrant wave from S2. Snapshots at time = 700 ms. (Aiv, Biv, and Civ) Snapshots of the re-entrant wave. Amiodarone terminated re-entrant wave. (Av, Bv, and Cv) Evolution of the AP of an EPI cell, respectively. (D and E) The dominant frequency. (F and G) The minimum spatial length of a premature S2

Acknowledgements

The authors thank Dr. Ismail Adeniran for useful discussions. This study was supported by the China Scholarship Council (CSC), the National Science Foundation of China (NSFC) under Grants No. 61571165 and No. 61572152, and Shandong Province Natural Science Foundation under Grant No. ZR2015FM028.

References

1. Brugada R, Hong K, Dumaine R, Cordeiro J, Gaita F, et al. (2004) Sudden death associated with short-QT syndrome linked to mutations in HERG. Circulation 109: 30-35.
2. Lu LX, Zhou W, Zhang X, Cao Q, Yu K, et al. (2006) Short QT syndrome: a case report and review of literature. Resuscitation 71: 115-121.
3. ten Tusscher KH, Panfilov AV (2006) Alternans and spiral breakup in a human ventricular tissue model. Am J Physiol Heart Circ Physiol 291: H1088-1100.
4. Luo C, Wang K, Zhang H (2017) In silico assessment of the effects of quinidine, disopyramide and E-4031 on short QT syndrome variant 1 in the human ventricles. PLoS One 12: e0179515.
5. Adeniran I, McPate MJ, Witchel HJ, Hancox JC, Zhang H (2011) Increased vulnerability of human ventricle to re-entrant excitation in hERG-linked variant 1 short QT syndrome. PLoS Comput Biol 7: e1002313.
6. McPate MJ, Duncan RS, Hancox JC, Witchel HJ (2008) Pharmacology of the short QT syndrome N588K-hERG K+ channel mutation: differential impact on selected class I and class III antiarrhythmic drugs. Br J Pharmacol 155: 957-966.
7. Lalevee N, Nargeot J, Barrere-Lemaire S, Gautier P, Richard S (2003) Effects of amiodarone and dronedarone on voltage-dependent sodium current in human cardiomyocytes. J Cardiovasc Electrophysiol 14: 885-890.
8. Gray DF, Mihailidou AS, Hansen PS, Buhagiar KA, Bewick NL, et al. (1998) Amiodarone inhibits the Na(+)-K+ pump in rabbit cardiac myocytes after acute and chronic treatment. J Pharmacol Exp Ther 284: 75-82.
9. Nishimura M, Follmer CH, Singer DH (1989) Amiodarone blocks calcium current in single guinea pig ventricular myocytes. J Pharmacol Exp Ther 251: 650-659.
10. Watanabe Y, Kimura J (2008) Acute inhibitory effect of dronedarone, a noniodinated benzofuran analogue of amiodarone, on Na+/Ca2+ exchange current in guinea pig cardiac ventricular myocytes. Naunyn Schmiedebergs Arch Pharmacol 377: 371-376.
11. Zankov DP, Ding WG, Matsuura H, Horie M (2005) Open-state unblock characterizes acute inhibition of I potassium current by amiodarone in guinea pig ventricular myocytes. J Cardiovasc Electrophysiol 16: 314-322.
12. Gima K, Rudy Y (2002) Ionic current basis of electrocardiographic waveforms: a model study. Circ Res 90: 889-896.
13. Szabo G, Szentandrassy N, Biro T, Toth BI, Czifra G, et al. (2005) Asymmetrical distribution of ion channels in canine and human left-ventricular wall: epicardium versus midmyocardium. Pflugers Arch 450: 307-316.

Address for correspondence.
Name: Cunjin Luo
Full postal address: Room 306, Integrated Laboratory Building, School of Computer Science and Technology, Harbin Institute of Technology, Xidazhi Street, Nangang District, Harbin, 150001, China.
E-mail address: cunjin.luo@yahoo.co.uk